

## Research Article

# Differences in Energy Consumption in Electric Vehicles: An Exploratory Real-World Study in Beijing

Kezhen Hu,<sup>1,2</sup> Jianping Wu,<sup>1</sup> and Tim Schwanen<sup>2</sup>

<sup>1</sup>Department of Civil Engineering, Tsinghua University, Beijing 100084, China

<sup>2</sup>Transport Studies Unit, School of Geography and the Environment, University of Oxford, Oxford, UK

Correspondence should be addressed to Kezhen Hu; [kezhen.hu@outlook.com](mailto:kezhen.hu@outlook.com)

Received 7 April 2017; Revised 4 July 2017; Accepted 6 August 2017; Published 13 September 2017

Academic Editor: Jing Dong

Copyright © 2017 Kezhen Hu et al. This is an open access article distributed under the Creative Commons Attribution License, which permits unrestricted use, distribution, and reproduction in any medium, provided the original work is properly cited.

Electric vehicles (EVs) are widely regarded as a promising solution to reduce air pollution in cities and key to a low carbon mobility future. However, their environmental benefits depend on the temporal and spatial context of actual usage (journey energy efficiency) and the rolling out of EVs is complicated by issues such as limited range. This paper explores how the energy efficiency of EVs is affected and shaped by driving behavior, personal driving styles, traffic conditions, and infrastructure design in the real world. Tests have been conducted with a Nissan LEAF under a typical driving cycle on the Beijing road network in order to improve understanding of variations in energy efficiency among drivers under different urban traffic conditions. Energy consumption and operation parameters were recorded in both peak and off-peak hours for a total of 13 drivers. The analysis reported in this paper shows that there are clear patterns in energy consumption along a route that are in part related to differences in infrastructure design, traffic conditions, and personal driving styles. The proposed method for analyzing time series data about energy consumption along routes can be used for research with larger fleets of EVs in the future.

## 1. Introduction

Among many innovative technologies to decarbonize urban transport, electrification of the vehicle fleet has been viewed by many as an effective way to reduce carbon emissions, energy consumption, air pollution, and oil dependence [1]. Electric vehicles (EVs) have the benefits of zero tailpipe emissions, low engine noise, and higher propulsion efficiency, and many local governments have demonstrated their commitment to electromobility, particularly in populated urban areas with severe air quality problems [2].

However, the energy consumption and air pollution during the generation of the electricity used to power EVs cannot be neglected. Although the substitution of EVs for internal combustion engine powered vehicles (ICEVs) can have huge environmental benefits with, for instance, reductions in GHG emissions of 33% in the USA [3], the effects will be (much) smaller in countries with a higher share of thermal power stations in electricity generation mix. Huo and colleagues [4] pointed out that, with China's current mix, the potential energy benefits are offset by the high pollution levels of coal-fired power plants. In regions like Northeastern China

(including Beijing), EVs could induce almost the same GHG emissions compared to ICEVs for the worst-case calculation.

Yet, the environmental benefits of EVs depend not only on electricity generation or even the production and afterlife of vehicles and batteries [5] but also on how EVs are used in actual driving conditions. This is an issue that remains poorly understood; researchers and policymakers have yet to appreciate fully how differences in driving behavior can cause variations in the energy efficiency of EVs, in part because of the low EV penetration in the urban vehicle fleet. The effects of driving behavior can be expected to be particularly important in geographical contexts where fossil fuels play an important role in the generation of electricity used to power EVs.

There has been research about reducing EV energy consumption in the usage phase that focuses on the vehicle side through, for instance, optimization of the powertrain system, upgrading of motor control strategy, and improvements in battery power density. Stockar et al. [6] presented a supervisory energy management strategy based on Pontryagin's minimum principle to optimize the energy utilization of a plug-in hybrid electric vehicle (PHEV) on a simulator.

Smith and colleagues [7] proposed a study of suitable battery size by characterizing urban commuters' profiles in a town in Canada. In addition to these approaches which have attracted considerable attention within the vehicle manufacturing industry, driving behavior itself could be a profoundly influential factor in reducing energy consumption in EV usage.

Driving behavior and driving styles, dispositions to drive in particular ways that have been acquired over time, have been shown to result in fluctuations of vehicle energy efficiency for conventional vehicles, where, for example, aggressive drivers can consume 30% more fuel [8]. Environmental-friendly driving, or eco-driving, has become a key topic of interest in the intelligent transport systems community for conventional vehicles. Eco-driving habits can also be expected to enable the EV motor to function in the high-efficiency region and fully tap the potential of the regenerative function to extend an EV's driving range. However, some research under laboratory conditions has suggested that EV motor efficiency is much less sensitive to speed and load than are internal combustion engines [9]. Together with the potential of EVs' regenerative braking function to reclaim the kinetic energy, the new EV features have raised doubts as to whether the benefits of congestion mitigation and eco-driving will be as prominent for EVs as for conventional vehicles.

Consequently, there is a gap in the literature regarding the impact of driving behaviors on EVs' energy consumption in the real-world operation phase. There have been some modeling and simulation of EVs with specific driving cycles such as ECE-15, FUDS, NYCC, and Japanese 10–15 mode cycle [10], but no study has so far examined if a single standardized driving cycle can capture the dynamics encountered in real-world urban driving conditions as well as the heterogeneity among drivers. Driving behaviors emerge out of the interplay of contextual conditions and person-specific driving styles, and both those behaviors and the interplay from which they emerge tend to fluctuate in the real world instead of staying the same. Therefore, we developed an observational experiment of driving behavior with EVs to study the variation in EV energy efficiency among different drivers in the Beijing context, which is one of the major emerging markets for EV adoption in China. The aim of our EV energy efficiency test is not only to study the impacts of drivers' behavior on energy consumption but also to explore the interplay of EV driving styles with road infrastructure and traffic conditions. To this end, a range of analysis methods are deployed to data at the levels of the whole trip and moments within each trip. These include a specific type of feature extraction method called Singular Spectrum Analysis (SSA) and clustering analysis using the Dynamic Time Warping (DTW) distance in order to maintain the sequential information in the energy consumption data during the analysis of driver heterogeneity along the test route.

The remainder of the paper is organized as follows. After a review of relevant literature on EV energy consumption, Section 3 introduces the experiment and the methodological approach for analysis. This is followed by analysis of results in Section 4 and finally conclusions in Section 5.

## 2. Literature Review

Research has sought to better understand and estimate the energy consumption of electric vehicles from different perspectives. One strand of research analyzes energy consumption through field tests on dedicated tracks. Cenex (the UK's center of excellence for low carbon and fuel cell technologies) has a test track composed of different parts to simulate four driving cycles, including a high-speed circuit, city course, hill route, and a handling route with a total length of 11.8 km [11]. Bingham et al. [12] conducted a field test on the Cenex test site to study energy consumption using a Smart Electric Drive EV. The field test excluded car-following behaviors and dynamic traffic conditions which are typical of urban driving. The authors pointed out that reducing the spread of vehicle acceleration has the potential to reduce energy consumption by 30%. However, microscale driving parameters were not thoroughly analyzed, and the analysis results were considered preliminary.

Another study on the same Cenex test site suggested that opportunities for regenerative energy capture were the largest on the high-speed circuit [13]. The results also showed that energy efficiency differed significantly among drivers. The high-speed circuit requires drivers to drive at full throttle but also offers many opportunities for deceleration, leading to remarkable changes in energy efficiency. The track test results also suggested a strong and positive relationship between regeneration ratio and journey energy efficiency (defined as the estimated vehicle range for each percentage of state of charge [SOC]) for both the high-speed and city circuits, with the latter simulating European cities with a speed limit of 48 km/h and numerous mandatory stops. However, real-world data collected in the UK as part of the Smart Move trial contradicted the track test results by showing a negative relationship. This discrepancy has triggered our interest in studying the impacts of driving behavior on EV energy consumption in real-world conditions.

Other than field tests, simulation is a feasible method in resource-constrained conditions for analysis. Zhang and Yao [14] proposed a driving strategy for when EVs approach a signalized intersection and estimated the energy consumption under different control strategies based on a VT-Micromodel for conventional vehicles. However, their model failed to capture the complexity of the regenerative function and the maneuver scheme also supposed a free driving behavior without interactions with other drivers. The result showed an 8% saving of energy compared to the baseline scenario.

Meanwhile, some authors have proposed a platform or model for EV energy consumption at a regional scale. Lee and Wu [15] developed an approach to estimate the driving range more accurately by the evaluation of both battery degradation and driving behavior. Four groups of driving behaviors, characterized by a vector of speed slots and relative percentage of energy consumption, were clustered according to an unsupervised machine-learning approach (growing hierarchical self-organizing maps). Unfortunately, this research neglected the importance of energy regeneration in driving behavior. Li et al. [16] identified six factors affecting the energy consumption and constructed a binary model to

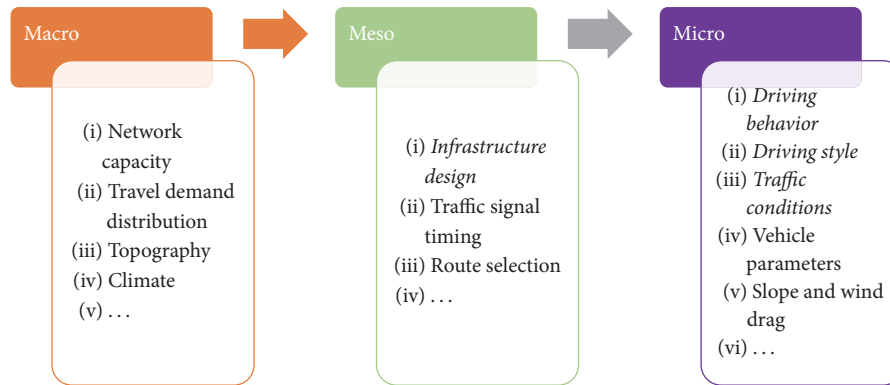


FIGURE 1: A hierarchical map of influencing factors for EV energy consumption (factors considered in the empirical study printed in italic).

carry out an empirical experiment in Sydney, by focusing on topography, infrastructure, traffic, and climate. However, the validated binary model was not readily transferable to areas other than Sydney, due to its context-specificity and oversimplification compared to a microscopic model with more parameters [14].

Notably, although largely neglected in behavior-oriented EV energy research, there has been a separate strand of studies focused on energy consumption in the vehicle heating, ventilation, and air-conditioning systems (HVAC) of EVs. To assess the geographical and environmental influence on energy consumption as well as the effect of preconditioning, Kambly and Bradley [17] put transient environmental parameters from the database into a thermal comfort model. The results showed that, due to different HVAC usage requirements, EV range varied widely across the geography as well as the time of day in the USA.

In sum, en-route EV energy consumption is a process affected by different factors on multiple levels (Figure 1). Previous research has seldom addressed the effects of meso- and microlevel factors on energy consumption in the real world. Understanding the effects of those factors is critical to better design of EV driving performance experiments in the future and can also feed into the development of specific eco-driving guidelines for EV users. This paper concentrates on three micro- and one mesolevel factor (i.e., driving behavior, driving style, traffic conditions, and infrastructure design) and how they affect energy consumption in EVs.

### 3. Experimental Design and Methodology

In this part, we first describe the design of the experiment in which energy consumption and other data were collected; then the methods used to analyze energy consumption are introduced.

#### 3.1. Experimental Design

**3.1.1. Test Equipment.** A battery electric vehicle Nissan LEAF 2011 model was used as the test vehicle. An On-Board Diagnostics (OBD) device data logger was connected to the vehicle Electronic Control Unit (ECU) along the actual

driving tests, and the data were later uploaded to a computer for analysis. The OBD provided second-by-second information including vehicle speed, motor torque, motor speed, battery pack current, and voltage. Derivative values such as instant acceleration and energy consumption could be calculated accordingly. A portable GPS was also used during the test to capture the location for each second, and ambient temperature data were recorded using an electric thermometer.

**3.1.2. Route.** In order to be representative of average daily driving behavior, the selected test route started from the residential area of Haidian District (near the 5th ring road) and ended in Sanlitun CBD (between the 2nd and 3rd ring road) in Chaoyang District. All the drivers were instructed to drive on the same route at the same time of day. This route to some degree simulates a typical daily commuting routine as employment is spatially concentrated in the inner area of Beijing. The test route contains multiple road types, including an arterial road, a bypass, an expressway, and a highway inside the 5th ring of Beijing. Figure 2 details the different road types and a map of the test route.

**3.1.3. Test Time.** Since morning peak hour is commonly defined as 7:00–9:00 a.m. in Beijing (e.g., [18]), the 8:30 a.m.–10:30 a.m. timeslot on weekdays covers both peak and off-peak hours and ensured that multiple traffic conditions were encountered during the test. The test roundtrip consists of a more congested departure trip (average around 50 min, starting at 8.30 a.m. for all drivers) and a smoother return trip (average around 30 min, starting after 9:45 a.m.). Statistics [19] showed a relatively stable daily pattern of traffic on the Beijing network on normal weekdays, indicating traffic conditions were similar (although not identical) for the different drivers. All the trials were carried out within two months from October 2015 and days of extreme weather (rain, wind) and special events were excluded.

**3.1.4. Drivers.** As pointed out in a survey carried out by Xing and colleagues [20], 63.4% of EV drivers in Beijing in 2015 were male and 36.6% were female. 79% of the drivers fell into the age group of 20–39, and the majority of the

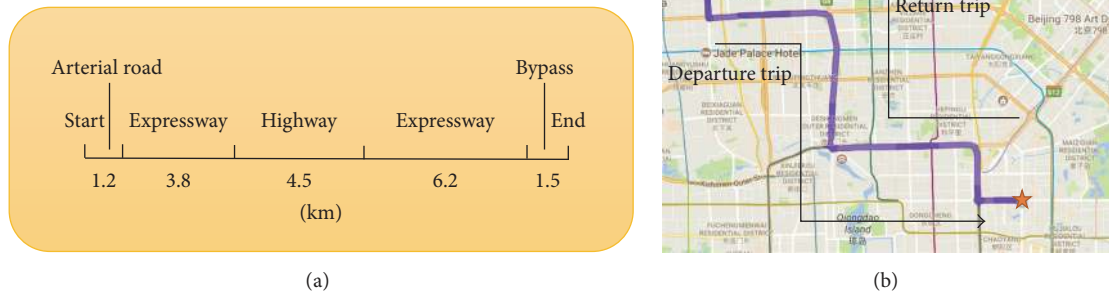


FIGURE 2: Road types (a) and map of the test route (b).

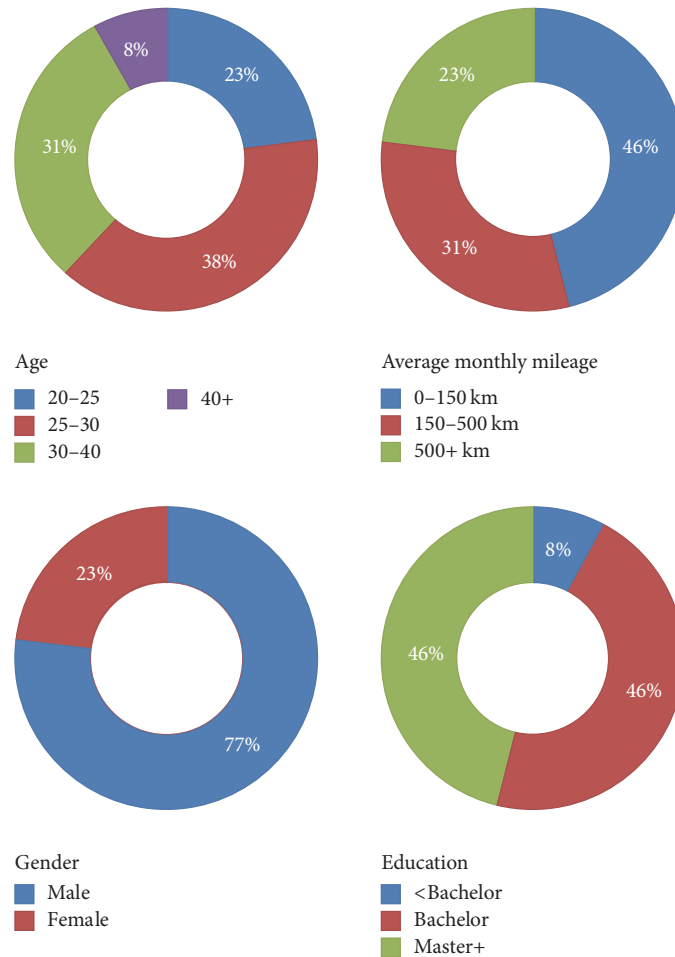


FIGURE 3: Drivers' background information.

EV drivers were well educated (with 68% of them gaining a bachelor degree or beyond, compared to 35.7% for all Beijing residents). To make the test result more representative of current EV drivers, we recruited trial participants with similar background characteristics as the survey had revealed using a snowball sampling method. A total of 13 drivers were selected and took part in the experiment. The majority of subjects in the experiment are well-educated young male adults who have driven an EV before (Figure 3).

**3.1.5. Test Conditions.** Although battery capacity might fade and increase impedance during cycling [21], we tried to limit the influence of battery performance by maintaining the same SOC at 80% at the beginning of each departure trip. Before the formal trial started, drivers were allowed extra time to get familiar with the test EV, and preconditioning was carried out until a preset level (80%) of SOC was reached. To ensure consistency, we used no additional “comfortable loads” (i.e., power consumption and user convenience features such as



air-conditioning and heating or radio) during the formal trials. It is noteworthy that, in contrast to the ideal conditions in a simulation platform or chassis test, the operation conditions could not be maintained at the same level in our research. We recognize the elements of uncertainty in our tests but believe they are inevitable when the aim is to obtain real-world, transient, and dynamic data for analysis.

**3.2. Methodology.** Traditional statistical tools, such as Mann-Whitney test and correlation analysis, can be used to analyze the characteristics of the whole trip for each driver but are less appropriate to examine the variation and autocorrelation in energy consumption along the route. The best way to identify patterns in energy consumption along the route for each individual in a manner that maintains the completeness of the dataset is to use feature extraction methods as applied in pattern recognition [22]. Feature extraction seeks to obtain the most important information from the original data and projects that information into a lower dimensionality space. Common feature extraction methods include Fourier Transform, Walsh-Hadamard Transform, and Wavelet Transform [22]. In our case, a meaningful decomposition of an observed time series into signal and noise components can provide a better understanding of the dynamics in energy consumption, especially in its relation to road environment and traffic conditions.

**3.2.1. Time Series Analysis Approach.** A relatively new method known as Singular Spectrum Analysis (SSA) is a powerful technique based on the decomposition of time series [23] and embedding theorem [24] and can be applied to any field with an interest in time series data, including hydrology, geophysics [25], climatology, economics, biology, and physics. The central idea of SSA is to decompose the sequence into a group of independent components, including trend, oscillating components (e.g., periodic effects), and uninformative noise. SSA is appropriate for this study because it makes no prior assumptions about whether the data is normally distributed or stationary [26] and the energy consumption sequence data in our study is quite dynamic with extensive autocorrelation and noise. Moreover, unlike Wavelet Transform, SSA does not require the selection of an appropriate basis wavelet based on the nature of the original data.

Detailed descriptions of the SSA algorithm are available elsewhere [26–28] but the basic methodological process that is used for extraction of the signals [29] can be summarized as follows.

For a standardized time series  $x_i$  with index  $i$  varying from  $i$  to  $N$  and a window length (or maximum lag)  $L$ , a Toeplitz lagged correlation matrix is formed by

$$C_j = \frac{1}{N-j} \sum_{i=1}^{N-j} x_i x_{i+j} \quad 0 \leq j \leq L-1. \quad (1)$$

The eigenvalues,  $\lambda_k$ , and eigenvectors,  $E_j^k$ , of the Toeplitz matrix are calculated and sorted in descending order of  $\lambda_k$ ,

where indices  $j$  and  $k$  vary from 1 to  $L$ . The  $k$ th principal component is

$$a_i^k = \sum_{j=1}^L x_{i+j} E_j^k \quad 0 \leq i \leq N-L. \quad (2)$$

Each component of the original time series identified by SSA can be reconstructed, with the  $k$ th reconstructed component (RC) series given by

$$x_i^k = \frac{1}{M} \sum_{j=1}^L a_{i-j}^k E_j^k \quad L \leq i \leq N-L+1. \quad (3)$$

$\lambda_k$  represents the fraction of the total variance of the original sequential data that the  $k$ th RC accounts for and RCs can be ordered by decreasing importance accordingly. Most of the variance is contained in the first few RCs and most or all of the remaining RCs contain noise.

**3.2.2. Clustering Method.** Given the high dimensionality of the spatial sequence data, it is highly beneficial to extract and visualize the structure of similarity and differences between the drivers. Clustering is a powerful tool to reveal and visualize the structure of data. The choice of methods for measuring similarities/dissimilarities has a significant impact on the clustering results. According to Izakian et al. [30], Dynamic Time Warping (DTW) distance is an appropriate indicator for use in shape-based clustering. The DTW function calculates an optimal match between two time series by stretching or compressing some segments of the series. Hence, this technique is suitable for measuring energy consumption patterns' similarity with respect to their shapes.

An agglomerative clustering method (Ward's Method) is used with DTW as the distance function. Ward's Method has been chosen because of its suitability for small datasets concerning robustness and efficiency compared to the  $k$ -means algorithm [31]. The general procedure of Ward's Method starts with each candidate as a separate cluster and then merges two clusters to produce the smallest increase in the sum of squares. The merging process goes on until it reaches  $k$  clusters [32]. While the  $k$ -means algorithm gives no guidance about what  $k$  should be, Ward's Method gives indications through the increases in merging cost at each step; a rule of thumb is to keep reducing  $k$  until the cost jumps and then use the  $k$  right before the jump. In our study, the DTW calculation and agglomerative clustering process are carried out after the standardization of each sequence into  $z$ -scores in MATLAB.

## 4. Results and Discussion

This section summarizes the results from our experiments and starts with statistical analysis of various characteristics at the level of the whole trip (temporal domain analysis). It then turns attention to variations in energy consumption between moments along the trial route (spatial domain analysis).

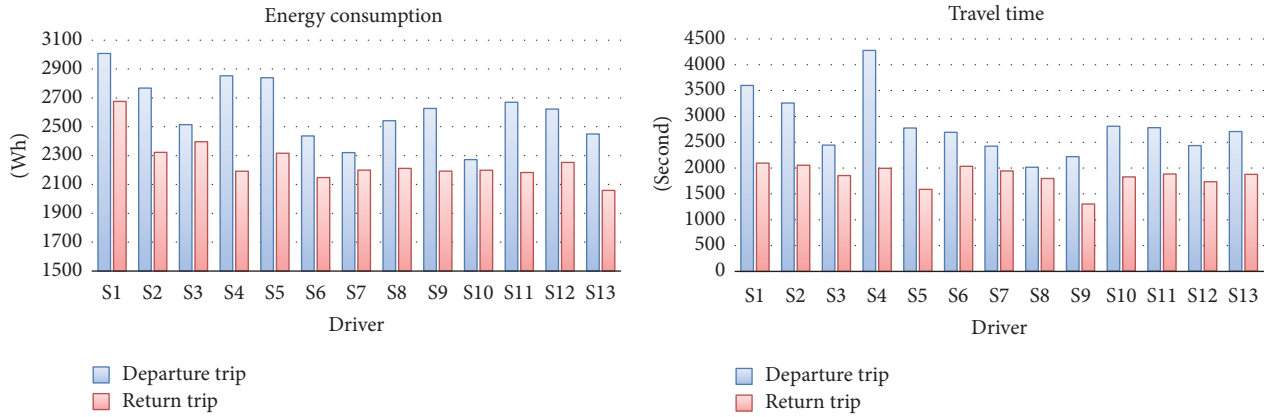


FIGURE 4: Energy consumption and time cost for all drivers.

**4.1. Temporal Domain Analysis.** Figure 4 demonstrates some initial results on travel time and energy consumption for each subject. The drivers' energy consumption varied slightly more during peak hour than at off-peak time. The maximum difference among all drivers (the worst-performing versus the best-performing driver) is 32.4% during peak hour and 30.0% at off-peak time. On average, the energy consumption during congested traffic conditions is 15.6% higher than during smooth conditions (2609.7 Wh and 2257.7 Wh, resp.), which is statistically significant at the 95% confidence level (Mann–Whitney  $U = 14$ ,  $p = 0.0001$ ). The coefficient of variation (defined as the ratio of the standard deviation to the mean) for energy consumption decreases from 2.3% in congested conditions to 1.9% in smooth conditions, while that of time decreases from 6.0% to 3.3%. Thus, during congested conditions, drivers display slightly larger variation in both energy consumption and time cost.

Real road traffic conditions affected vehicles during the driving process, which included repeated episodes of start, acceleration, deceleration, and stop operations. The trip was divided into four types of driving status: acceleration, deceleration, constant speed, and idling. The idling mode is defined as the condition in which the battery power is turned on to supply the motor although the actual vehicle speed is 0; the acceleration mode is defined by the acceleration speed  $a > 0.2 \text{ m/s}^2$  in the constant driving process; deceleration mode happens when acceleration goes below  $a < -0.2 \text{ m/s}^2$  in the constant driving process; and the constant speed mode is defined as instantaneous acceleration  $|a| < 0.2 \text{ m/s}^2$ , while speed is above 0. Episodes (series of continuous moments) of each status have been aggregated across individual trips. The distribution of these four types of driving status as the percentage of total number of episodes is shown for each driver in Figure 5. The difference of idling share between the two traffic conditions is pronounced (3.8% for the departure trip in congested conditions versus 1.8% for the return trip in smooth conditions).

The average total number of episodes of acceleration, deceleration, constant speed, and idling were 214, 206, 309, and 30 for the departure trip (peak hour) and 145, 140, 218, and 9 for the return trip (off-peak). As shown in the

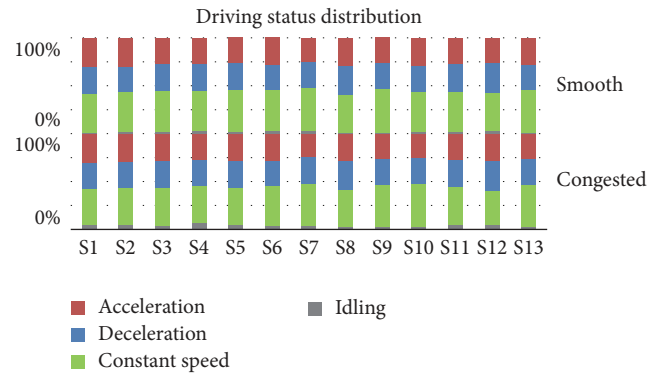


FIGURE 5: Driving status distribution for all drivers.

TABLE 1: Mann–Whitney test for episode frequency by driving status according to traffic condition (congested versus smooth).

	Congested	Smooth	$p$ value (2-tailed)
Number of idling episodes	30	9	0.000
Number of constant speed episodes	309	218	0.001
Number of deceleration episodes	206	140	0.000
Number of acceleration episodes	214	145	0.001

Mann–Whitney test in Table 1, there are statistically significant (5% level) differences in all the four statuses, which indicates a much more continuous driving behavior with smoother traffic.

Although the lateral comparison does not indicate a strong positive relation between acceleration share and energy consumption, the longitudinal comparison for individual drivers does give some hints. The driver (S5) with the largest change in energy consumption between the smooth (off-peak) trip and the peak congested (peak hour) trip (decrease by 18.4%) showed a decrease in total deceleration and acceleration shares with 2.0 percentage points.

TABLE 2: Pearson's correlation coefficients for various trip attributes, by road traffic conditions.

Congested	Energy consumption	Travel time	Acc share	Dec share	Const share	Idling share	Energy regeneration	Average Acc	Average Dec	Ambient temperature
Energy consumption	1.00									
Travel time	0.32	1.00								
Acc share	0.70**	0.39	1.00							
Dec share	0.04	-0.43	0.13	1.00						
Const share	-0.54	-0.35	-0.81**	-0.54	1.00					
Idling share	0.29	0.82**	-0.40	-0.14	-0.59*	1.00				
Energy regeneration	0.56	0.02	0.72**	0.61*	-0.82**	0.20	1.00			
Average Acc	0.75*	0.21	0.82**	0.43	-0.87**	0.42	0.89**	1.00		
Average Dec	0.55	-0.01	0.64*	0.51	-0.74**	0.24	0.84**	0.78**	1.00	
Ambient temperature	0.40	0.10	0.32	-0.05	-0.15	-0.00	0.35	0.43	-0.01	-0.18
Smooth	Energy consumption	Travel time	Acc share	Dec share	Const share	Idling share	Energy regeneration	Average Acc	Average Dec	Ambient temperature
Energy consumption	1.00									
Travel time	0.26	1.00								
Acc share	0.36	0.46	1.00							
Dec share	0.21	-0.12	-0.23	1.00						
Const share	-0.43	-0.35	-0.48	-0.67*	1.00					
Idling share	-0.17	0.36	-0.49	0.03	-0.01	1.00				
Energy regeneration	0.59*	0.33	0.59*	0.45	-0.77**	-0.33	1.00			
Average Acc	0.49	0.35	0.63*	0.38	-0.75**	-0.33	0.93**	1.00		
Average Dec	0.18	0.16	0.19	0.65*	-0.73**	0.01	0.75**	0.69**	1.00	
Ambient temperature	0.40	0.44	0.52	-0.14	-0.20	0.32	0.57*	0.38	0.27	1.00

\*\*Correlation is significant at the 0.01 level (2-tailed); \*Correlation is significant at the 0.05 level (2-tailed).

In contrast, the driver with the smallest change in energy consumption (\$10, decrease by 3.3%) displayed an increase of the summed deceleration and acceleration shares with 3.0 percentage points in the smooth trip.

Correlation analysis has been conducted to obtain a better understanding of the relationships between energy consumption and other trip attributes and among the latter (Table 2). The coefficients show a weak linear relationship ( $r = 0.32$  for peak hour traffic and  $r = 0.26$  for off-peak, where neither is significant at the 5% level) between energy consumption and travel time, which reinforces the earlier conclusion that no simple relation can be identified between trip time and trip energy consumption for a specific route in real-world urban driving conditions. In congested conditions, the constant share has a stronger negative correlation with energy consumption ( $r = -0.54$ ) than during smooth conditions ( $r = -0.43$ ), yet neither correlation is significant at the 5% level. In peak hour traffic, a higher acceleration share tended to come with higher energy consumption than at off-peak time ( $r = 0.70$  against  $r = 0.36$ ). Average acceleration is also less strongly correlated with average deceleration when traffic is

less congested (which is quite intuitive, since the driver will have more control and freedom when traffic is reduced and smooth). Ambient temperature was not significantly correlated with other factors except for a positive correlation ( $r = 0.57$ ) with energy regeneration in smooth traffic. Since the variation of ambient temperature across all the 13 trials was within 8°C, we will disregard the impacts of temperature in the remainder of this study.

The energy regeneration ratio is positively correlated with acceleration and deceleration share ( $r = 0.72$  and  $r = 0.61$ , both significant at the 5% level), but higher energy recovery does not guarantee less energy consumption, given that more energy regeneration caused by deceleration will require acceleration to adapt to traffic flow speed. To better illustrate this pattern, the journey energy efficiency (defined as in [13] with the unit of km/SOC) and the regeneration ratio (regenerative energy/consumed energy) have been plotted in Figure 6. As the figure shows, journey energy efficiency is more strongly correlated with the regeneration ratio during congested traffic than in smooth conditions. Both the regeneration ratio and the journey energy efficiency tended to be higher for off-peak

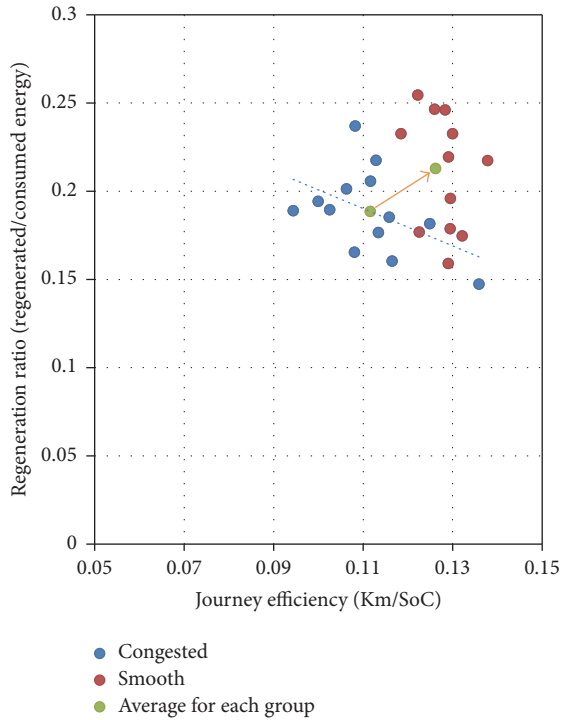


FIGURE 6: Regeneration ratio versus journey energy efficiency by traffic conditions.

trips. The following “spatial domain analysis” part will try to explain the underlying fact for the “energy regeneration conundrum” from a geographical point of view.

**4.2. Spatial Domain Analysis.** High-resolution spatial data on energy consumption has rarely been studied directly before due to the limited availability of the data in the case of conventional vehicles. However, the highly electrified system in EVs makes it possible to record instant energy consumption based on battery pack current and voltage. This data can be used to examine how driving behaviors and styles, traffic conditions, and infrastructure conditions such as road curvature, traffic signals, and exits affect energy consumption along the trial route.

As a first step of analysis, we have plotted the geographical distribution of averaged speed and energy consumption (and the respective standard deviations) along the route for the 13 drivers in Figure 7. The temporal sequential energy consumption and speed data were converted into spatial sequential data through the integration of On-Board Diagnostics (OBD) and GPS data for the congested trip towards CBD and the smooth return trip separately. The speed profile is steadier under smooth than congested traffic conditions. Due to the functioning of the regenerative brake, energy consumption fluctuated more strongly than did speed.

As described in Section 3.2, the Singular Spectrum Analysis (SSA) method is applied to the spatial sequence analysis. A spatial resolution of 0.1 km was chosen for aggregation after weighing data compression against data integrity. Sensitivity analysis of different aggregation lengths on SSA results has

also been conducted (in response to the Modifiable Areal Unit Problem (e.g., [33]) according to which measuring phenomena at different spatial scales can result in radically different conclusions), showing that 0.1 km resolution yielded a good result.

An appropriate window length  $L$  needs to be chosen for the SSA.  $L$  should be large enough to capture sufficiently the dynamics of the time series but not greater than  $N/2$  [34]. Further, if any periodic component is known to be present, then  $L$  should be proportional to that period. In practice, a length approximately  $1/5$  of the sequence is sufficient to capture all the dynamics of the series. To the best of the authors’ knowledge, there have been no previous studies using datasets that are very similar to ours. Therefore, based on our understanding of the designated route which comprises several signals, entrance, and exits (a distance of less than 1 km in the arterial road) and changes in road curvature, a window length of 30 (namely, 3 km because our resolution is 0.1 km) was chosen in our case.

Let us use as an example to illustrate the SSA process with the departure trip data of driver S10. We have used MATLAB to perform the SSA. Choosing  $L = 30$  and performing SVD of the correlation matrix  $C_j$ , we obtain 30 eigenvectors, ordered by their contribution (share) in the decomposition (see Figure 8).

The drop in values around component 8 could be interpreted as the start of the noise floor. Together the first eight components account for 83.3% of the variation in the original sequence. The respective reconstructed components for the first eight components are shown in Figure 9.

RC 1 represents the slowly varying trend component which excludes oscillations. Based on the closeness of corresponding eigenvalues and the similarity in frequency, RC 2, RC 3, RC 4, and RC 5 are paired as the harmonic components which show the pattern of periodic oscillation in the original series. The harmonic component could probably be interpreted as the periodic impact of interferences, including recurrent congestion points. The rest of the eigenvectors are categorized as noise. Figure 10 shows the extracted components of the three categories.

This SSA process was performed twice for each driver and for all 13 drivers separately to extract the trend component which we define as the main feature of interest for each driver. The harmonic component is correlated with the trend component to a certain degree, yet of a much more versatile nature. In the present study, we focus only on the trend component which accounts for over 60% of the variation in the original sequential data.

After extracting the trend components of energy consumption for each individual, the DTW calculation and agglomerative clustering process are carried out with the standardized values ( $z$ -scores) of each sequence in MATLAB. The dendrograms for the clustering results for both congested and smooth traffic conditions are plotted in Figure 11. The rescaled merging cost on the horizontal axis shows greater heterogeneity in energy consumption along the route among drivers during smooth (off-peak) traffic than during congested peak hour conditions. For the congested condition, merging driver S4 with other groups involved a high cost and



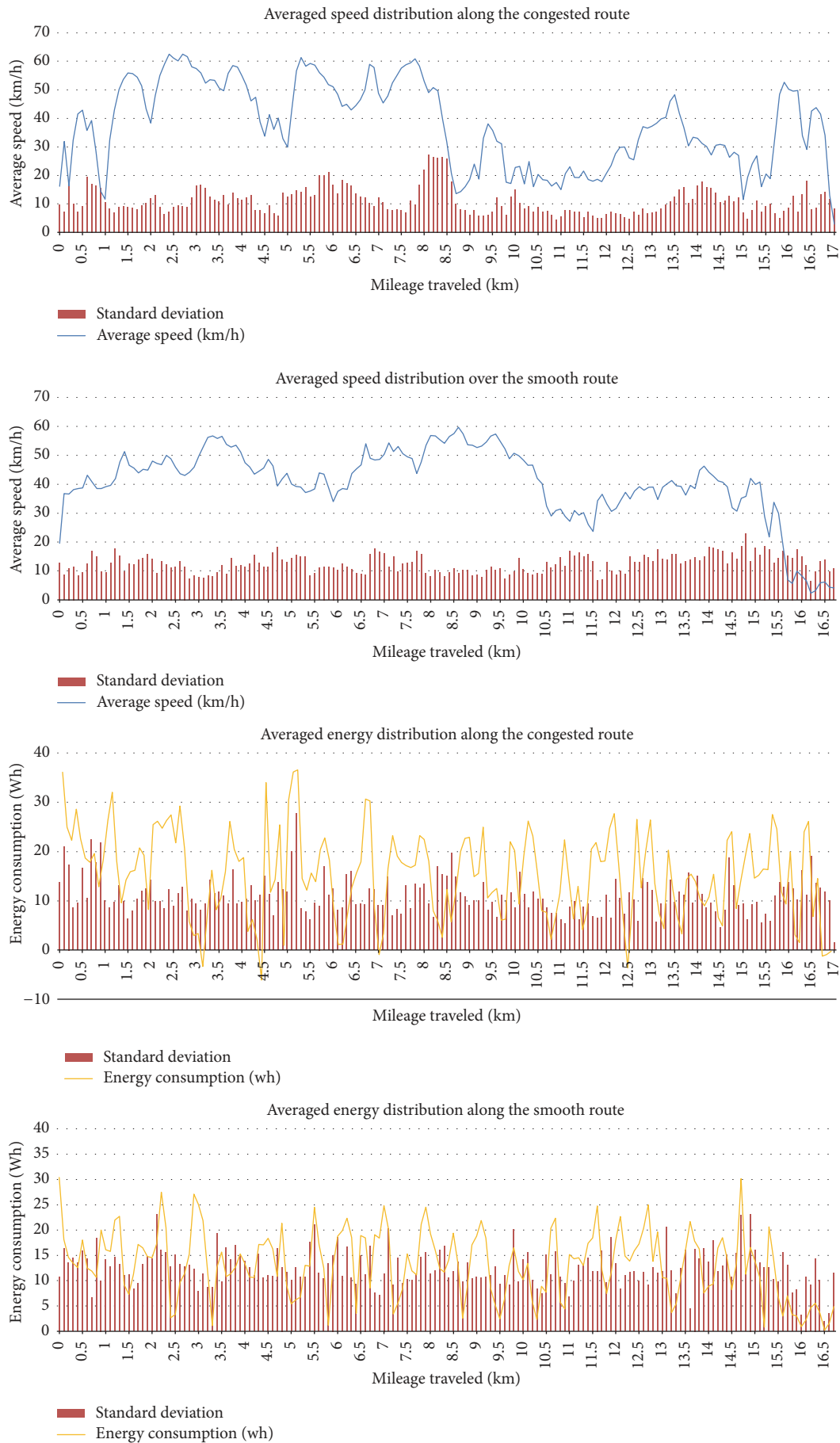


FIGURE 7: Speed and energy distribution along the route.

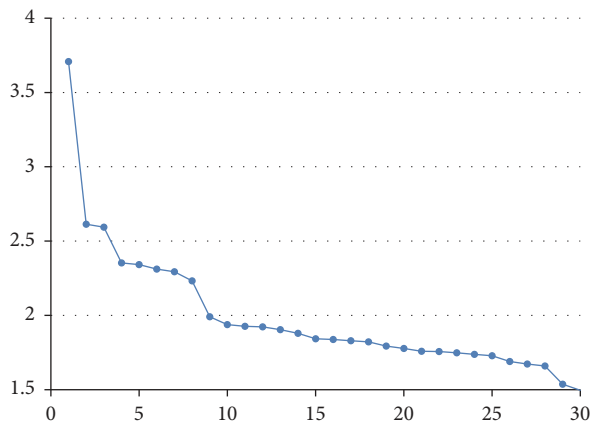


FIGURE 8: Logarithms of the 30 eigenvalues.

other groups were more closely nested. We used a rescaled merging cost of 5 as the cut-off value and decided to cluster drivers into three groups and one anomaly (S4). For the smooth condition, we used the same cut-off value of 5 to obtain three groups and two anomalies (S7, S4). Among all the drivers, only two pairs (S5 and S12, S7 and S10) remain in the same group in both sets of conditions. This suggests that traffic condition strongly influences individual energy consumption pattern along the route in ways that a focus on the total energy consumption during the trip may not necessarily reveal.

The energy consumption profiles ( $z$ -scores) along the trial route for the different groups during congested conditions are shown in Figure 12. The overall trend for the clusters shows a fluctuation with different peak locations for each cluster. They all start with high levels of energy consumption and then exhibit a dramatic plunge, followed by more modest decrease until approximately 5 km for clusters A and B and until 9.5 km for Cluster C. The initial decline is in line with the shifting from densely signalized road type (arterial road in and bypass) to expressway, which is also the case in the smooth return trip. Clusters A and C have subsequent peaks around 9.5 and 13 km, respectively; most drivers in B maintain a fairly flat or slightly increasing profile until the end of the drive. The shape for S4 is really different and further analysis suggested that this driver experienced much more extensive congestion with travel speeds below 10 km/h around the peak in Figure 12(d).

The energy consumption profiles ( $z$ -scores) along the trial route for the different groups in the smooth conditions are plotted in Figure 13. All clusters fluctuate in a similar “W” shape although the depth of the troughs varies. Energy consumption decreases steadily in all clusters for the first 1.5 km (similar to the congested condition as a result of densely signalized road type). Then Cluster B remains stable until further decreasing starts at around 7.0 km, while Cluster A and Cluster C continue with the declining trend at different rates. All three clusters peak at the same point and then experience rapidly falling energy consumption until they reach a minimum around 10.5 km after which the energy consumption rises again. The outliers S4 and S7 do not fit in with

other clusters; retrieved speed profiles reveal that the abnormal energy consumption peaks are associated with severe “speed valleys” around 7.5 km and 11.5 km, respectively, which are not present for other drivers. Intragroup heterogeneity is generally larger than in the congested condition, probably because the recurrent congestions during peak hours place more constraints on drivers’ driving behavior. Hence, similar drivers tend to converge in terms of revealed driving behaviors.

To better understand the differences in energy consumption profile, we have mapped both the original energy consumption (the sum of the trend, harmonic, and noise components) and speed along the route for each cluster using QGIS (Figures 14 and 15). For the speed plots, the crimson color denotes high speeds up to 80 km/h, while the primrose color denotes low speeds down to 10 km/h. As for the energy consumption plots, the blue color represents energy regeneration up to 25 Wh, and the red color represents energy consumption with a maximum value of 70 Wh. Road sectors with negative energy consumption values are defined as “net energy regeneration sectors.”

Figure 14 confirms that different clusters of drivers show quite different patterns of energy consumption. The peaks and valleys revealed in Figure 12 largely coincide with changes in road curvature and road types. All the three clusters display a decreasing trend in energy consumption when the drivers move from the densely signalized arterial road sector to the relatively smoother expressway. Then the three clusters begin to diverge at the change point to the highway. Cluster A and Cluster C continue the decreasing trend in energy consumption, while drivers in Cluster B peak shortly after entering the highway. The retrieved speed profile shows that Cluster B drivers encounter slightly more severe congestion when entering the highway and subsequently rapidly increase their speed. Also, Cluster B drivers display more aggressive driving behaviors after they enter into the highway at the very beginning.

When departing from the highway and entering the expressway again, drivers in all clusters show a decrease in speed because the complex signalized intersection linking the highway to the expressway is a bottleneck. The energy consumption trend of Cluster A peaks near this bottleneck as the speed shows that it encounters a longer congested length compared to the other two clusters. After drivers enter the expressway again, the continuous low speed results in low energy consumption in all clusters. While clusters A and B maintain a constant trend until the end of the journey, energy consumption in Cluster C peaks at the bending point of the expressway (north 3rd ring road and east 3rd ring road). This pattern of Cluster C can be attributed to a lack of proactive slowing down behavior followed by “stop-and-go” driving in the congested sectors.

The occurrence of a net energy regeneration road sector (blueish sector) is always associated with a peak in the energy consumption profile (Figure 12). This partly solves the “energy regeneration conundrum” mentioned in Section 4.1. Higher regenerated energy comes at the cost of using more energy to speed up and regain free-flow speed. The efficiency improvement brought by EV motors and the regenerative

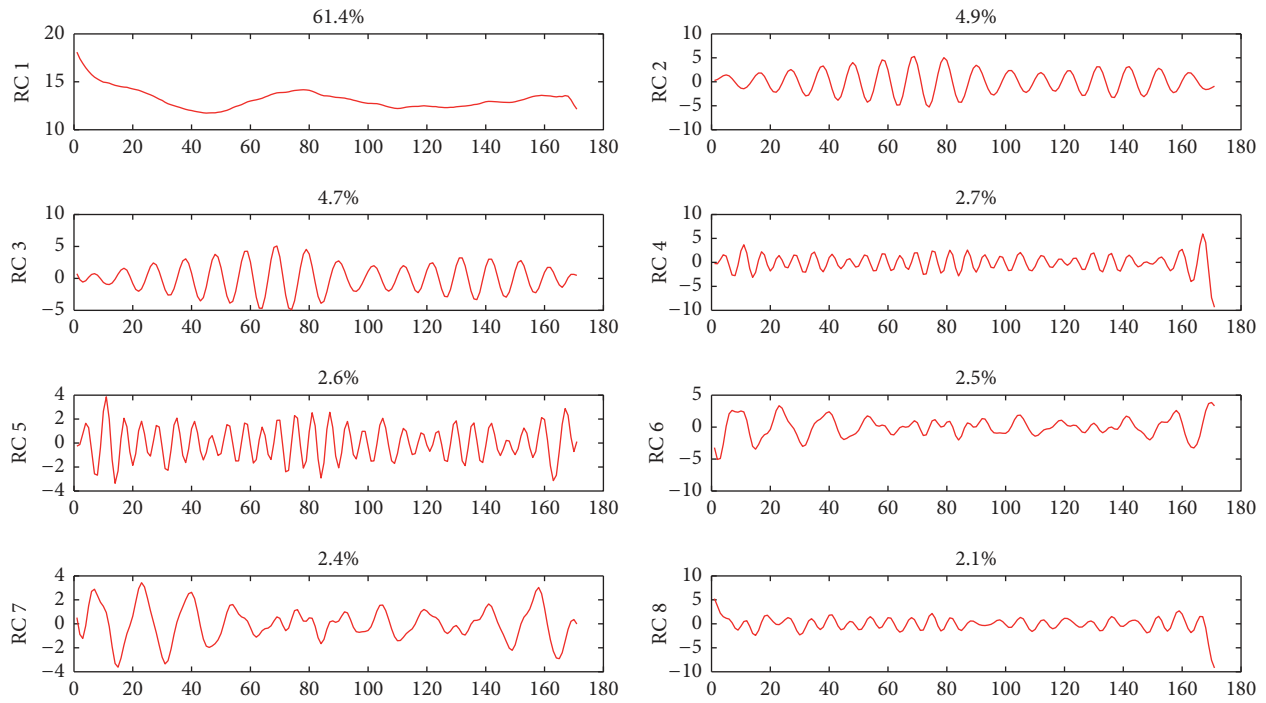
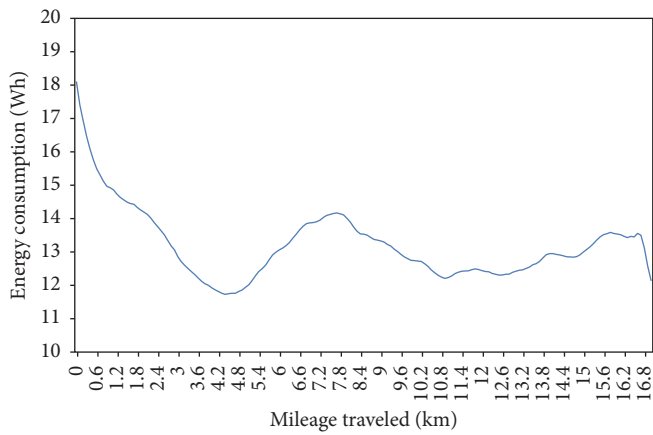
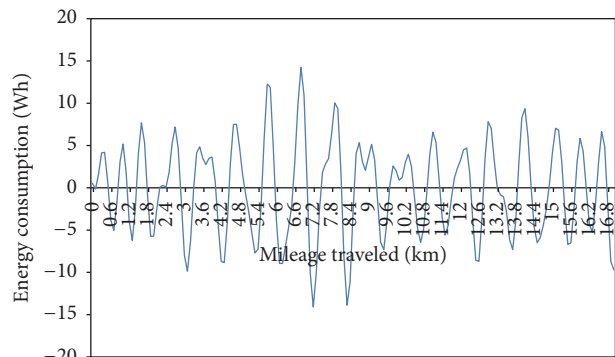


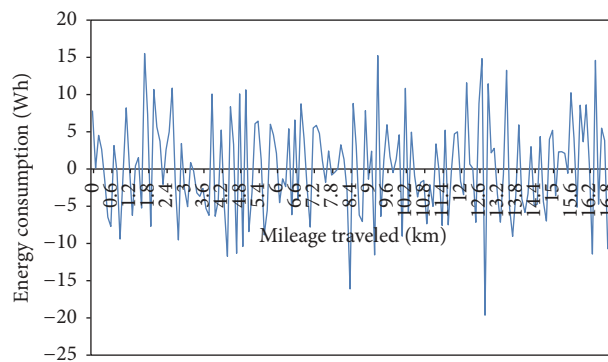
FIGURE 9: The first eight reconstructed components plotted as time series.



(a)



(b)



(c)

FIGURE 10: Reconstructed trend (a), harmonic (b), and noise (c).

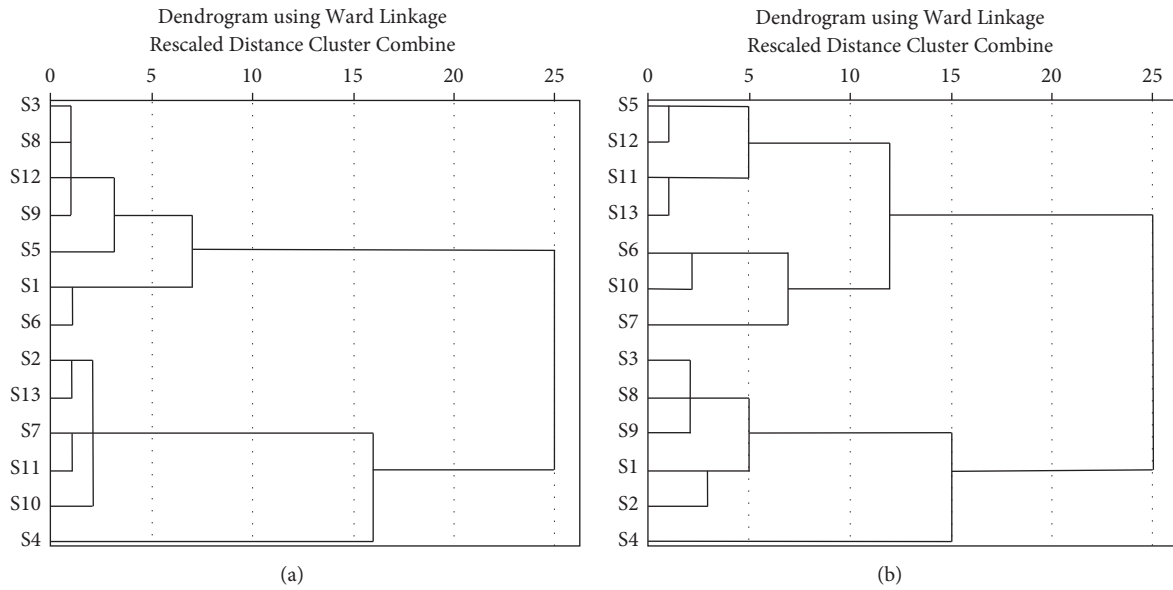


FIGURE 11: Dendrograms of the clustering results, congested (a) and smooth (b).

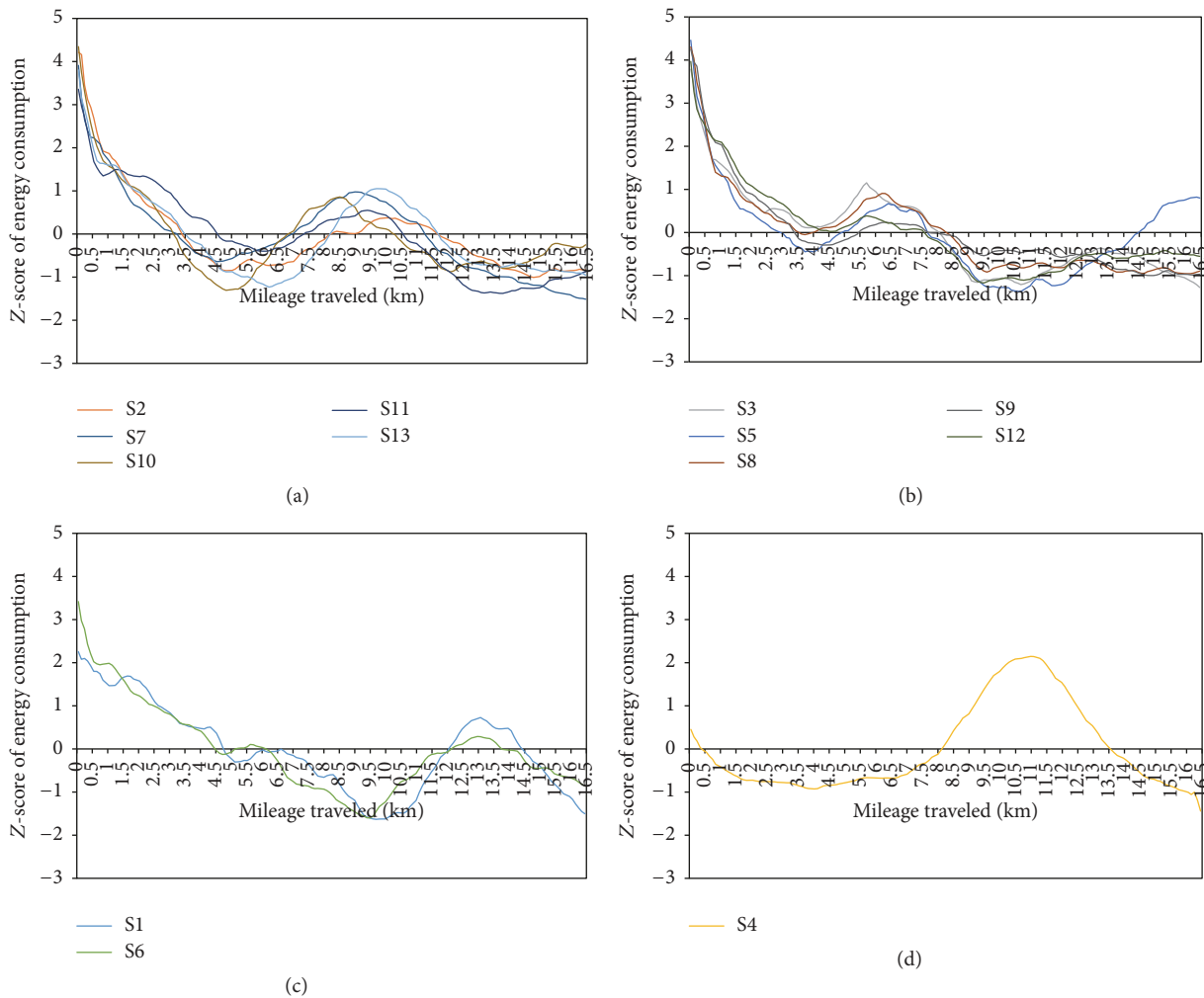


FIGURE 12: Energy consumption pattern for different clusters in congested traffic condition: (a) Cluster A: S2, S7, S10, S11, and S13; (b) Cluster B: S3, S5, S8, S9, and S12; (c) Cluster C: S1 and S6; (d) anomaly: S4.



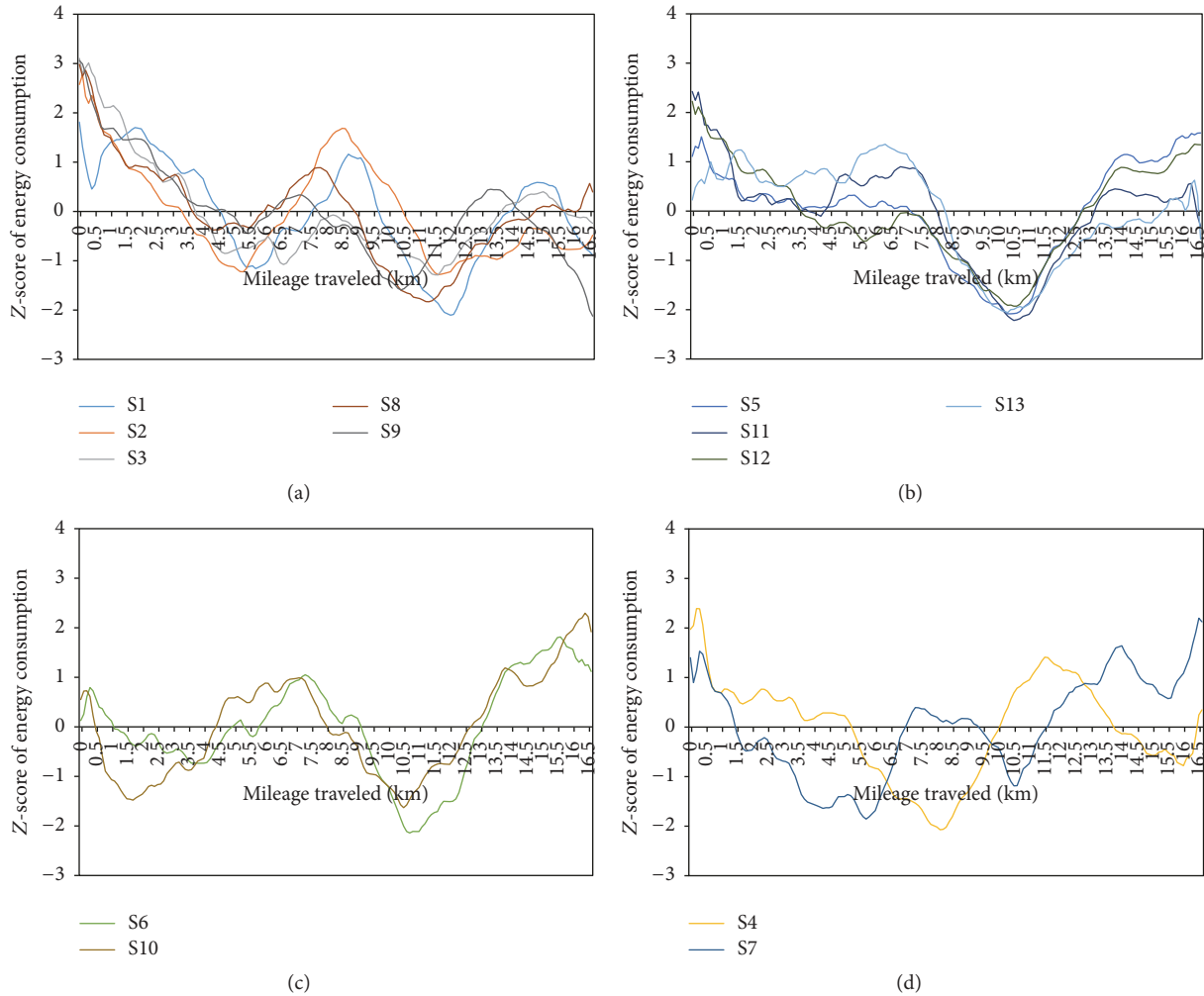


FIGURE 13: Energy consumption pattern for different clusters in smooth traffic condition: (a) Cluster A: S1, S2, S3, S8, and S9; (b) Cluster B: S5, S11, S12, and S13; (c) Cluster C: S6 and S10; (d) anomaly: S4 and S7.

function has not annihilated the influence of “stop-and-go” driving behavior.

In smooth traffic conditions (Figure 15), the patterns are not as obvious as during peak hour. The overall intragroup difference in energy consumption is larger than during peak hour. All the three clusters reach their lowest energy consumption around the exit of the highway to the expressway. Cluster A peaks roughly at the middle point of the highway sector due to drivers driving at high speeds for the longest time span. Cluster B has the longest plateau in energy consumption with a mild and consistent driving profile. Cluster C performs quite efficiently at the start of the journey; in fact, it keeps a mild speed profile until it reaches the bending point of the expressway, after which its pattern becomes similar to Cluster B.

It is worth mentioning that net energy regeneration sectors occur less often in smooth than in congested traffic conditions. While a freer driving environment might be expected to induce more variation in energy consumption, this is not borne out in our experiment. The setting for urban driving in megacities like Beijing is always quite constrained

(speed limit, traffic signal, road curvature, road safety regulations, etc.), so the speed profile cannot be manipulated to the same extent as on test tracks as in previous research [13]. In fact, the most significant contributor to the energy consumption pattern seems to be “stop-and-go” driving incurred during congested traffic conditions, which subsequently results in even larger variation among drivers.

### 5. Conclusions

This paper has introduced an exploratory experiment of EV driving behavior which was undertaken to understand the variation of EV energy efficiency among different drivers in Beijing context. It is among the first attempts to systematically compare real-world spatial sequence data on energy consumption for EV drivers, and the approaches put forward in the paper can be used for data from large-scale EV fleets in the future. The significant heterogeneity among drivers’ revealed energy consumption along the trial route, which is not captured in the statistical results at the level of the total journey, meriting further attention in future research with a

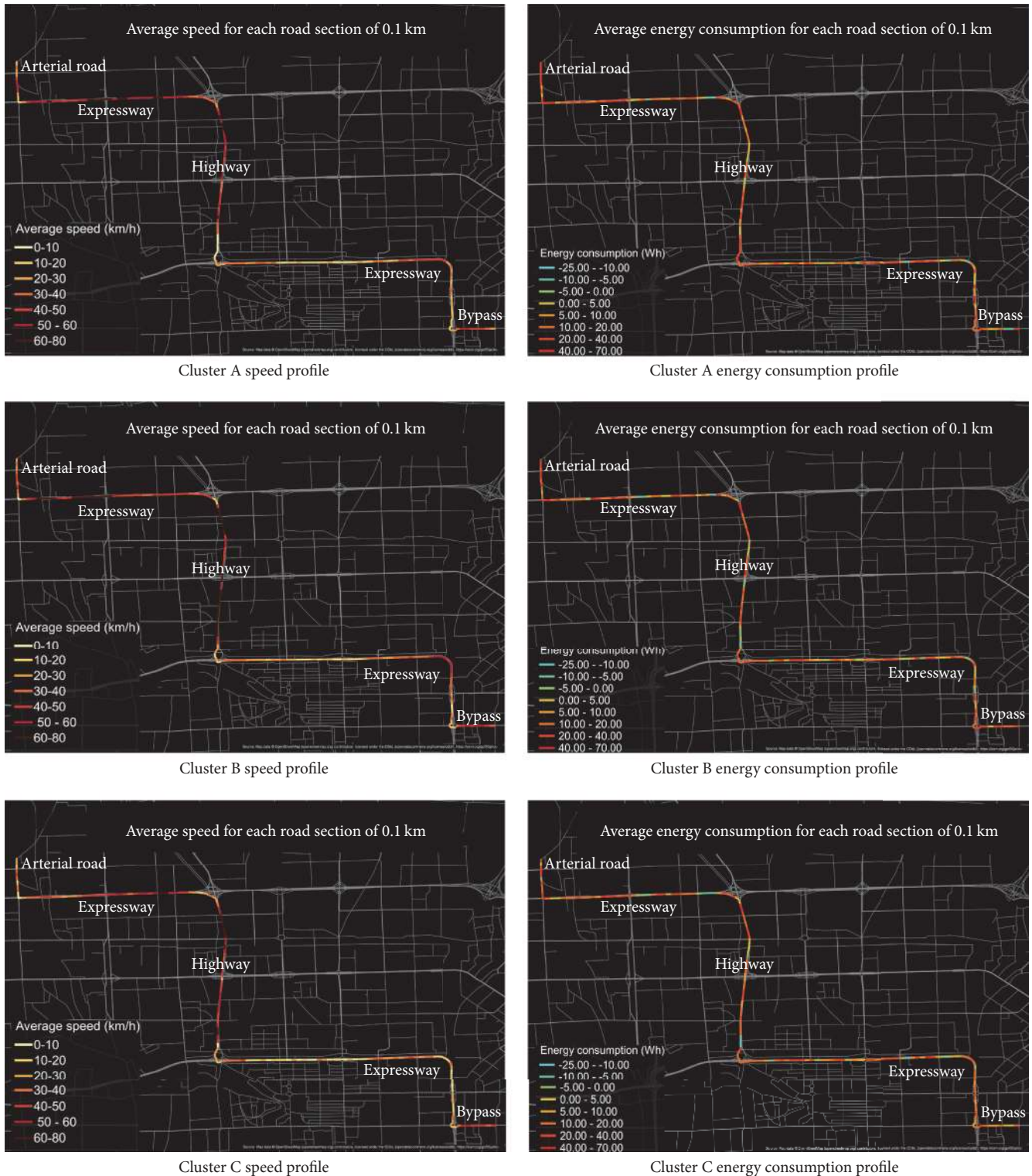


FIGURE 14: Speed and energy consumption profiles for different clusters in congested condition.

larger and more diverse fleet of EVs and greater numbers of drivers.

The paper has made two more specific contributions to the existing literature. First, it has shown that in combination

the SSA method and agglomerative clustering using the DTW distance offer a feasible approach to simplify and decipher the heterogeneity in energy consumption profiles that are present in sequential but seemingly erratic data. Second, both

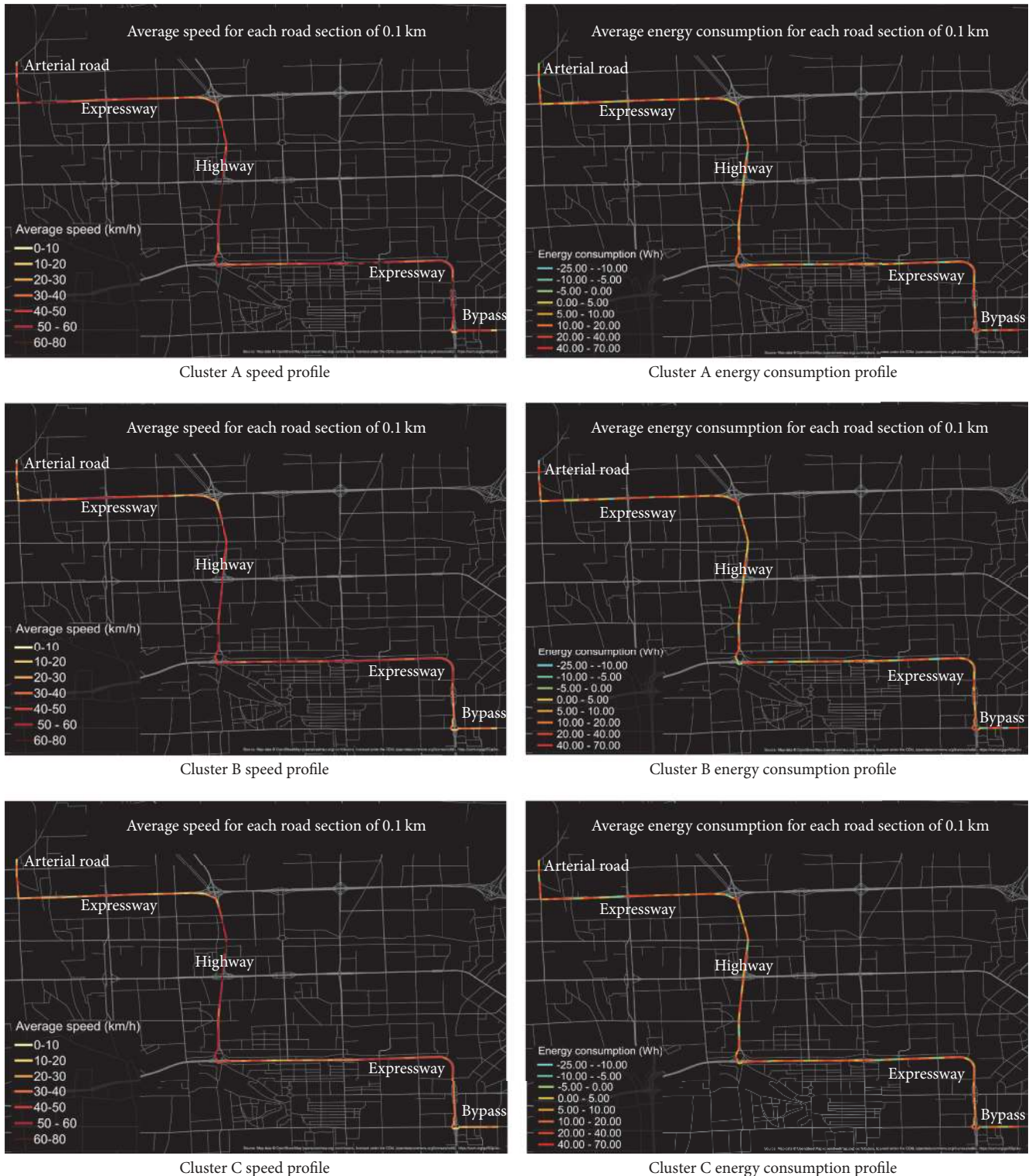


FIGURE 15: Speed and energy consumption profiles for different clusters in smooth condition.

the SSA method-based analysis and the earlier correlation analysis have revealed how energy efficiency is affected clearly by drivers' behavior and through this by road infrastructure (e.g., type of road, curvature), traffic conditions (congestion),

and personal driving styles. Of particular interest is that more heterogeneity exists among drivers in the same cluster in relatively smooth traffic than in congested, peak hour conditions. This suggests that recurrent congestion during



peak hours places more constraints on driving behavior so that drivers with similar driving styles tend to converge in revealed driving behavior.

The analysis reported in this paper is unable to differentiate the impacts of the physical environment (recurrent congestion, road curvature) from those of individual-specific driving style. Nevertheless, a certain degree of consistency is observed in the driving behavior of more energy efficient drivers under different traffic conditions. While the study has not directly focused on the analysis of eco-driving behavior, the results are in line with the claim that eco-driving can have substantial influence on energy consumption in EVs (which usually are more energy efficient than ICEVs). In contrast, it seems likely that the “energy regeneration ratio” is a poor indicator of eco-driving. The use of energy regenerative function may bring about more local-scale net energy regeneration sectors on a particular trip, but this benefit is always associated with an overall trend of increased energy consumption. Our results imply that behavioral change in driving can lead to substantial energy efficiency improvements, even in EV fleets. It is particularly in congested traffic conditions where the benefits of EV eco-driving can be reaped.

The findings of this research point out the importance for car manufacturers to estimate the driving range more accurately by including personal driving style factor, infrastructure design, and traffic condition factors in the calculations and projections of EV energy consumption. Providing such information may help to overcome range limitations among drivers and assist them to modify their driving habits. It may also increase public trust in information on EV performance that is provided by manufacturers.

## Conflicts of Interest

The authors declare that there are no conflicts of interest regarding the publication of this article.

## Acknowledgments

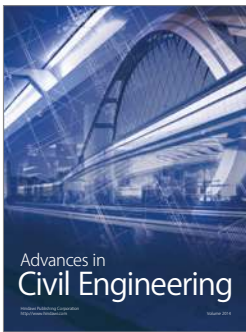
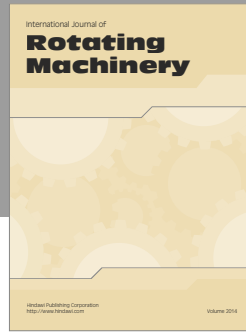
The authors acknowledge the support from Nissan (China) Investment Co., Ltd., which provided the test vehicle for this study. The authors would also like to thank Mr. Simon Abele from School of Geography and the Environment, University of Oxford, for his help in the visualization of the spatial data. An early version of this work was presented at the 5th European Battery, Hybrid and Fuel Cell Electric Vehicle Congress (EEVC 2017).

## References

- [1] C. Silva, M. Ross, and T. Farias, “Evaluation of energy consumption, emissions and cost of plug-in hybrid vehicles,” *Energy Conversion and Management*, vol. 50, no. 7, pp. 1635–1643, 2009.
- [2] International Energy Agency, “Global EV Outlook: understanding the electric vehicle landscape to 2020,” 2013.
- [3] T. Hodges and J. Potter, “Transportation’s Role in Reducing U.S. Greenhouse Gas Emissions Volume 1: Synthesis Report,” 2010.
- [4] H. Huo, Q. Zhang, M. Q. Wang, D. G. Streets, and K. He, “Environmental implication of electric vehicles in china,” *Environmental Science and Technology*, vol. 44, no. 13, pp. 4856–4861, 2010.
- [5] International Energy Agency, “Global EV Outlook 2016,” 2016.
- [6] S. Stockar, V. Marano, M. Canova, G. Rizzoni, and L. Guzzella, “Energy-optimal control of plug-in hybrid electric vehicles for real-world driving cycles,” *IEEE Transactions on Vehicular Technology*, vol. 60, no. 7, pp. 2949–2962, 2011.
- [7] R. Smith, S. Shahidinejad, D. Blair, and E. L. Bibeau, “Characterization of urban commuter driving profiles to optimize battery size in light-duty plug-in electric vehicles,” *Transportation Research Part D: Transport and Environment*, vol. 16, no. 3, pp. 218–224, 2011.
- [8] D. L. Greene and S. E. Plotkin, “Reducing greenhouse gas emission from US transportation,” Arlington: Pew Center on Global Climate Change, 2011.
- [9] T. Burress, “Benchmarking state-of-the-art technologies,” in *Proceedings of the 2013 US DOE Hydrogen and Fuel Cells Program and Vehicle Technologies Program Annual Merit Review and Peer Evaluation Meeting*, Oak Ridge National Laboratory (ORNL), Oak Ridge, Tenn, USA, 2013.
- [10] C. Chaiyamanon, A. Sripakagorn, and N. Noomwongs, “Dynamic modeling of electric tuk-tuk for predicting energy consumption in bangkok driving condition,” *SAE Technical Papers*, vol. 1, 2013.
- [11] S. Carroll and C. Walsh, “UK Electric Vehicle Case Studies,” SAE Technical Paper 2011-39-7225, 2011.
- [12] C. Bingham, C. Walsh, and S. Carroll, “Impact of driving characteristics on electric vehicle energy consumption and range,” *IET Intelligent Transport Systems*, vol. 6, no. 1, pp. 29–35, 2012.
- [13] C. Walsh, S. Carroll, and A. Eastlake, “UK electric vehicle range testing and efficiency maps,” SAE Technical Paper 2011-39-7224, 2011.
- [14] R. Zhang and E. Yao, “Eco-driving at signalised intersections for electric vehicles,” *IET Intelligent Transport Systems*, vol. 9, no. 5, pp. 488–497, 2015.
- [15] C.-H. Lee and C.-H. Wu, “A Novel Big Data Modeling Method for Improving Driving Range Estimation of EVs,” *IEEE Access*, vol. 3, pp. 1980–1993, 2015.
- [16] W. Li, P. Stanula, P. Egede, S. Kara, and C. Herrmann, “Determining the main factors influencing the energy consumption of electric vehicles in the usage phase,” in *Proceedings of the 23rd CIRP Conference on Life Cycle Engineering, LCE’16*, pp. 352–357, Berlin, Germany, May 2016.
- [17] K. Kambly and T. H. Bradley, “Geographical and temporal differences in electric vehicle range due to cabin conditioning energy consumption,” *Journal of Power Sources*, vol. 275, pp. 468–475, 2015.
- [18] H. Wang, X. Zhang, and M. Ouyang, “Energy consumption of electric vehicles based on real-world driving patterns: A case study of Beijing,” *Applied Energy*, vol. 157, pp. 710–719, 2015.
- [19] Beijing Traffic Index, 2015, <http://www.nitrafficindex.com>.
- [20] Y. Xing, G. Tal, Y. Wang et al., “A comparison of plug-in electric vehicle markets between china and the U.S. based on surveys,” in *Blue Book of New Energy Vehicles*, pp. 314–338, 2016.
- [21] J. Vetter, P. Novák, M. R. Wagner et al., “Ageing mechanisms in lithium-ion batteries,” *Journal of Power Sources*, vol. 147, no. 1-2, pp. 269–281, 2005.



- [22] G. Kumar and P. K. Bhatia, "A detailed review of feature extraction in image processing systems," in *Proceedings of the Fourth International Conference on Advanced Computing & Communication Technologies*, Rohtak, India, 2014.
- [23] M. Loève, *Probability Theory II*, Springer-Verlag, New York, NY, USA, 4th edition, 1978.
- [24] F. Takens, "Detecting strange attractors in turbulence," in *Dynamical systems and Turbulence*, D. A. Rand and L. S. Young, Eds., vol. 898 of *Lecture Note in Mathematics*, pp. 366–381, Springer, Berlin, Germany, 1981.
- [25] D. Kondrashov and M. Ghil, "Spatio-temporal filling of missing points in geophysical data sets," *Nonlinear Processes in Geophysics*, vol. 13, no. 2, pp. 151–159, 2006.
- [26] D. H. Schoellhamer, "Singular spectrum analysis for time series with missing data," *Geophysical Research Letters*, vol. 28, no. 16, pp. 3187–3190, 2001.
- [27] R. Vautard, P. Yiou, and M. Ghil, "Singular-spectrum analysis: a toolkit for short, noisy chaotic signals," *Physica D: Nonlinear Phenomena*, vol. 58, no. 1–4, pp. 95–126, 1992.
- [28] A. L. Rukhin, "Analysis of Time Series Structure SSA and Related Techniques," *Technometrics*, vol. 44, no. 3, pp. 290–290, 2002.
- [29] H. Hassani, "Singular spectrum analysis: methodology and comparison," *Journal of Data Science*, vol. 5, no. 2, pp. 239–257, 2007.
- [30] H. Izakian, W. Pedrycz, and I. Jamal, "Fuzzy clustering of time series data using dynamic time warping distance," *Engineering Applications of Artificial Intelligence*, vol. 39, pp. 235–244, 2015.
- [31] M. Kaur and U. Kaur, "Comparison between k-means and hierarchical algorithm using query redirection," *International Journal of Advanced Research in Computer Science and Software Engineering*, vol. 3, no. 7, 2013.
- [32] M. R. Anderberg, *Cluster Analysis for Applications: Probability and Mathematical Statistics: A Series of Monographs and Textbooks*, Academic Press, Cambridge, Mass, USA, 1973.
- [33] T. Cheng and M. Adepeju, "Modifiable temporal unit problem (MTUP) and its effect on space-time cluster detection," *PLoS ONE*, vol. 9, no. 6, Article ID e100465, 2014.
- [34] C. Beneki, B. Eeckels, and C. Leon, "Signal extraction and forecasting of the UK tourism income time series: a singular spectrum analysis approach," *Journal of Forecasting*, vol. 31, no. 5, pp. 391–400, 2012.



**Hindawi**

Submit your manuscripts at  
<https://www.hindawi.com>

